Journal of Electrotechnology, Electrical Engineering and Management (2023)
Clausius Scientific Press, Canada
DOI: 10.23977/jeeem.2023.060408
ISSN 2560-6697 Vol. 6 Num. 4

Research on Voltage Control Strategy of DC Microgrid System

Yutong Shi, San Li*

Wuhan Maritime Communication Research Institute, Wuhan, 430079, Hubei, China
**Corresponding author*

Keywords: DC microgrid; photovoltaic unit; energy storage; coordinated control

Abstract: New energy sources such as solar energy, tidal energy, and geothermal energy possess characteristics of random dispersion, making centralized utilization unfeasible. Microgrid structures and control methods are relatively simple, enabling rational utilization of new energy sources, and have garnered widespread attention. Compared to AC microgrids, DC microgrids are easier to control, reduce energy conversion steps, eliminate factors like reactive power, and maintain frequency consistency. Thus, they are more conducive to the efficient utilization and coordinated control of new energy. This paper investigates the coordinated control strategy of a photovoltaic and energy storage-based DC microgrid system. By assessing the range of bus voltage and the power balance between photovoltaic output and load absorption within the system, a coordinated operational approach for the photovoltaic-energy storage DC microgrid is proposed. Segregating the system into various operating states based on different control methods for photovoltaic units and energy storage, the system's operation becomes more efficient and economical. This further validates the feasibility of the proposed strategy.

1. Introduction

In practical life, electrical energy primarily stems from traditional sources like oil and coal. However, the utilization of these sources simultaneously inflicts irreversible harm to the environment. Faced with increasingly dire circumstances, experts and scholars have turned their attention towards new energy sources such as solar energy, wind energy, and geothermal energy. These new energy sources possess characteristics of renewability and environmental harmlessness, holding the potential to address the scarcity of electrical energy. Yet, the inherent drawbacks of new energy, including random dispersion and inadequate energy density, hinder their large-scale integration into conventional power grids, preventing them from fully demonstrating their attributes of cleanliness, efficiency, and flexible usage [1-3].

Microgrids offer a significant solution to the challenges posed by the large-scale integration of new energy sources, providing an essential means for the scaled application of distributed power sources. Consequently, microgrids have gained widespread adoption. When interconnected with the main grid, energy storage devices within a DC microgrid can adjust their generation capacity according to the main grid's needs and store and utilize electrical energy [4-6].

The objective of this study is to focus on a photovoltaic and energy storage-based DC microgrid.

The study places particular emphasis on refining battery control methods and overall coordinated control strategies. This work constructs a mathematical model for photovoltaic units and investigates charging and discharging strategies based on a generic model for energy storage. Operating modes are segregated based on control methods for photovoltaic units and energy storage, proposing a coordinated control strategy for the photovoltaic-energy storage DC microgrid. Segmentation into different modes is based on bus voltage values and system power balance, with distinct unit control methods for each mode, ultimately achieving high-efficiency system operation.

2. Microgrid Mathematical Model and Control Objectives

2.1 Photovoltaic and Energy Storage Unit

Solar energy is abundantly present in nature and is considered a new energy source due to its advantages of easy accessibility, cleanliness, and high efficiency. According to statistics up to the year 2025, photovoltaic capacity could reach 4600GW, accounting for approximately 16% of human electricity demand. As the external environment is constantly changing, modeling and characteristic analysis of photovoltaic units are necessary to maximize the energy output from photovoltaic units[7].

Photovoltaic cells can convert light energy into electrical energy. The practical equivalent circuit of a photovoltaic cell is illustrated in Figure 1. According to Kirchhoff's current law:

$$I = I_{ph} - I_d + \frac{U + IR_s}{R_{sh}} \tag{1}$$

where, I represents the output current, I_{ph} represents the photocurrent, and I_d represents the current flowing through the diode; U is the output voltage, R_s is the series resistance, and R_{sh} is the parallel resistance.

The relationship between the current I_d and the forward bias voltage $U_d = U + IR_s$ in the diode is given by:

$$I_d = I_0 \left\{ exp\left[\frac{q(U + IR_s)}{AKT} \right] - 1 \right\} \tag{2}$$

where, I_0 is the reverse saturation current, q is the charge ($1.6 \times 10^{19} C$), K is the Boltzmann constant, T is the temperature of the photovoltaic panel, and A is the diode's ideality factor, which typically ranges from 1~2. Substituting equation (2) into equation (1), the output current formula for the photovoltaic cell can be derived as follows:

$$I = I_{ph} - I_0 \left\{ exp\left[\frac{q(U + IR_s)}{AKT} \right] - 1 \right\} - \frac{U + IR_s}{R_{sh}} \tag{3}$$

Formula (3) can be simplified as:

$$I = I_{ph} - I_0 \left\{ exp\left[\frac{q(U + IR_s)}{AKT} \right] - 1 \right\} \tag{4}$$

The output voltage formula can be obtained according to equation (4) as follows:

$$U = \frac{AKT}{q} ln\left(\frac{I_{ph} - I_L}{I_0} + 1 \right) \tag{5}$$

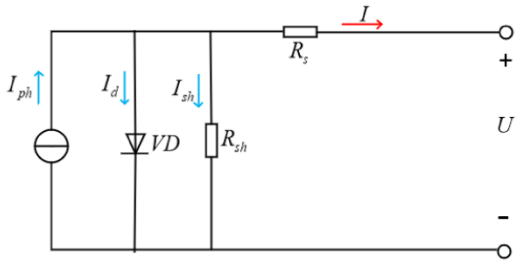

Figure 1 Equivalent circuit of photovoltaic cell

2.2 Energy Storage Unit (Battery)

The energy storage device in this study is a battery, which constitutes a central component of the DC microgrid. Batteries can store excess energy when the load power demand is low and release stored energy to compensate for system requirements during peak consumption periods. Batteries are commonly categorized based on their materials, including lead-acid and lithium-ion batteries. In this study, lithium-ion batteries are employed as the energy storage devices [8].

Lithium-ion batteries consist of four main components: the positive electrode, negative electrode, electrolyte, and separator. The operational principle involves the insertion and extraction of lithium ions into and from the positive and negative electrode materials. When an external electric field is applied to the battery, Li+ ions are extracted from the positive electrode, passing through the electrolyte and separator, and finally embedded in the negative electrode, resulting in a charging state. Conversely, during discharging, Li+ ions move from the negative electrode to the positive electrode [9]. Battery modeling and the study of its operational characteristics adopt a three-order dynamic model for the equivalent circuit, as depicted in Figure 2.

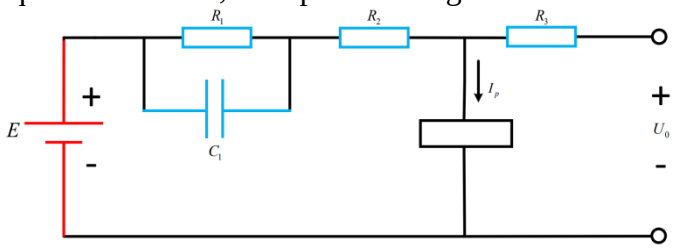

Figure 2 Third-order equivalent model of storage battery

In Figure 2, R_1 represents the diffusion resistance, R_2 is the transfer resistance, and R_3 signifies the polarization resistance. C_1 stands for the diffusion capacitance, and I_p represents the current in the branch. This model can reasonably simulate the charging and discharging processes of the battery. Based on this equivalent model, the equation for the output voltage u_{bat} can be derived as follows:

$$u_{bat} = E - R_{eq} i_{bat} \tag{6}$$

where, E is the DC voltage source, R_{eq} is the equivalent internal resistance, and i_{bat} is the output current. In the application of battery equivalent model, SOC value should also be considered. SOC refers to the percentage of the remaining power in the battery to the total power, which is defined as follows:

$$SOC = \frac{Q_r}{C_e} \tag{7}$$

Q_r represents the remaining charge, and C_e is the total charge. And equation (7) can also be

expressed as follows:

$$SOC = 1 - \frac{Q_u}{C_e} \tag{8}$$

In equation (8), Q_u represents the discharged amount of the battery. There are various methods for measuring the state of charge (SOC), including ampere-hour counting, open-circuit voltage method, and internal resistance method. This paper combines the charge accumulation method with the open-circuit voltage to calculate the SOC. Firstly, the open-circuit voltage of the battery is measured, and then the current and initial state of charge are calculated. SOC_0 represents the initial state of charge. The state of charge is then calculated using the charge accumulation method. Taking the battery i as an example, the calculation formula is as follows:

$$SOC_i = SOC_0 - \frac{\int_0^t i_{batt}\, d_t}{C_{batt}} \tag{9}$$

i_{batt} represents the output current, and C_{batt} denotes the capacity of the battery.

For the charging mode, this paper employs a two-stage charging method. This method involves using a constant current charging mode in the early stages of charging to accelerate the charging process. Once the voltage gradually rises to a constant value, the charging mode switches to constant voltage charging, avoiding potential damage to the battery caused by excessive current.

3. Direct Current Microgrid System Voltage Control Strategy

3.1 Coordinated Control Strategy for the System

This paper primarily investigates coordinated control methods for photovoltaic-energy storage DC microgrids to stabilize voltage and balance system power. Determining the switching manner of DC microgrid operational modes can enhance system stability. Figure 3 depicts a typical energy flow diagram of a microgrid system, where P_{pv} represents photovoltaic output power, P_l is the total load power, and P_b signifies battery output power.

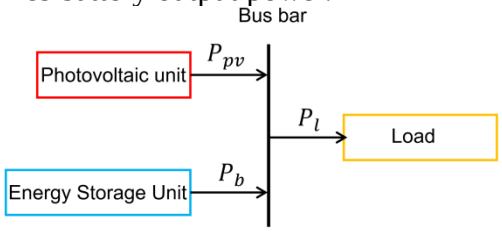

Figure 3 Block diagram of system energy flow

As can be seen from Figure 3, the following formula can be obtained during the stable operation of the system.

$$\sum_{i}^{m} P_{pvi}(t) + \sum_{j}^{n} P_{bj}(t) - \sum_{k}^{q} P_{lk}(t) = 0 \tag{10}$$

where m, n, and q represent the quantities of photovoltaic units, batteries, and loads respectively; $P_{pvi}(t)$ denote the photovoltaic unit i, $P_{bj}(t)$denote the power of battery j, and $P_{lk}(t)$ denote the power consumption of the load k.

In a photovoltaic-energy storage DC microgrid, photovoltaic units play a primary role as micro-sources, while batteries function similarly to micro-sources by stabilizing bus voltage and

maintaining power balance. Batteries can also act as loads, absorbing excess electrical energy generated by the photovoltaic units. During system operation, photovoltaic units switch between maximum power tracking and constant voltage modes, while energy storage units have both charging and discharging states [10].

Based on monitoring bus voltage u_{dc}, photovoltaic output power P_{pv}, and total load power P_l, the system can be classified into the following five operational states:

(1) If $630V > u_{dc} > 600V$, $P_l < P_{pv}$, photovoltaic units are in constant voltage mode, and batteries are charged using a two-stage method. Photovoltaic output power is reduced to maintain power balance and stabilize bus voltage.

(2) If $600V > u_{dc} > 570V$, $P_l < P_{pv}$, photovoltaic units transition from constant voltage output to maximum power output mode. Batteries store excess energy using compound droop control to stabilize DC bus voltage.

(3) If $570V > u_{dc} > 540V$, $P_l < P_{pv}$, photovoltaic units continue operating in maximum power output mode, and battery charging ceases.

(4) If $540V > u_{dc} > 510V$, $P_l > P_{pv}$, photovoltaic units operate in maximum power output mode, and batteries discharge using compound droop control. This collaborative operation ensures energy balance and stable bus voltage.

(5) If $510V > u_{dc} > 480V$, $P_l > P_{pv}$, and the battery discharge can't match the required load power, battery discharge is halted. Photovoltaic units continue to output power at maximum capacity, while non-essential loads are disconnected to stabilize voltage and maintain power balance.

3.2 Analysis of Operational Conditions under Different Circumstances

This paper will consider two scenarios that can lead to power imbalance within the microgrid system: (1) if the P_{pv} changes, while load power remains constant over a certain period, and photovoltaic output changes with external conditions; (2) if the P_l changes, and photovoltaic units maintain constant output power over a certain period, unaffected by external environmental conditions, with only the load power changing.

To study these scenarios, this paper establishes a simulation model for a direct current microgrid system, as illustrated in Figure 4. Set $\mathrm{T} = 25℃$, $S = 25W/m^2$, the maximum output power P_{pv} is $25kW$, and the rated voltage and capacity of the batteries are $300\mathrm{V}$ and $6.5\mathrm{Ah}$ respectively.

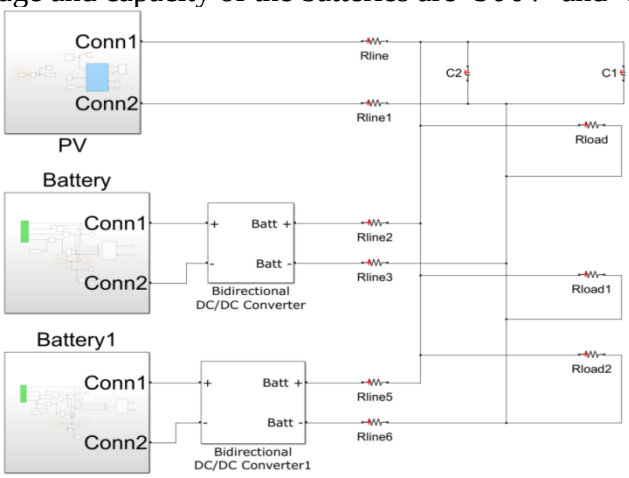

Figure 4 Simulation diagram of photovoltaic storage DC microgrid operation

3.2.1 Analysis of operating characteristics when photovoltaic output power changes

Assuming that the load power remains unchanged for a certain period of time, and the photovoltaic output power will change with the change of external environmental conditions, the first load power is set to $P_{load} = 12kW$, and the two loads are parallel at the same time, and their values are set to $P_{load1} = 6kW$ and $P_{load2} = 4kW$, then the total load power is $P_l = 22kW$.

(1) State 1

Setting $T = 25℃$, the light intensity $S = 900W/m^2$, $S = 1000W/m^2$ when $t = 0s$ and $t = 1s$ respectively, SOC is 90%, and the total simulation time is $3s$ (Figure 5).

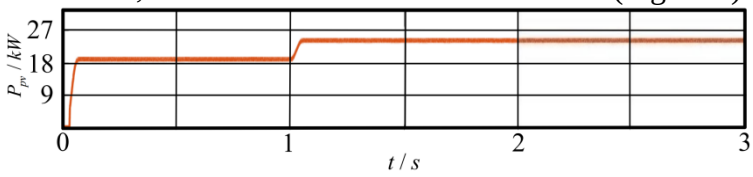

Figure 5 Photovoltaic power waveform

Figure 6 is the simulation diagram of photovoltaic output voltage u_{pv}, bus voltage u_{dc} and battery output current I_{b1}. It can be seen from the figure that when the photovoltaic unit is output at constant voltage, the variation range of U_{pv} is not large; The battery is in the two-stage charging mode, and the bus voltage is stable at about $600V$.

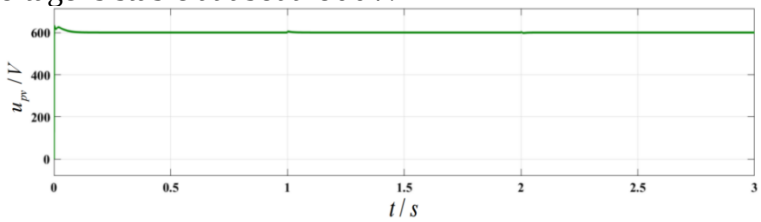

(a) Photovoltaic output voltage

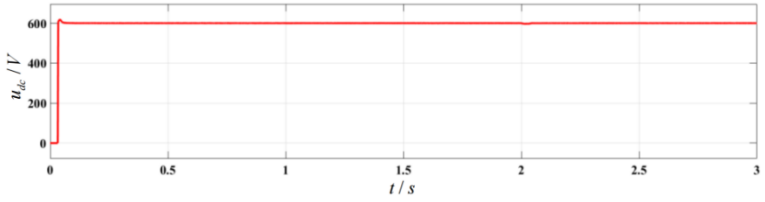

(b) Bus voltage

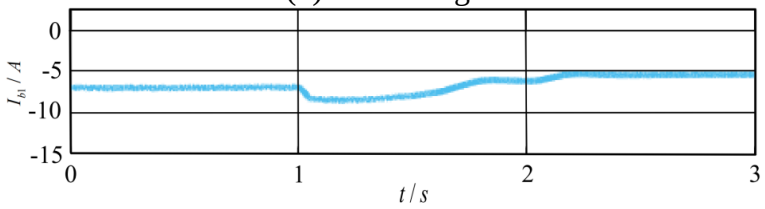

(c) Battery output current waveform of storage battery

Figure 6 The simulation diagram of photovoltaic output voltage, bus voltage and battery output current

(2) State 2/3/4

In state two, state three and state four, the battery is respectively in the composite droop charge, stop charge and composite droop discharge mode, while the photovoltaic cell has been in the maximum power output mode. Setting $T = 25$, the light intensity $S = 800, 900, 1000, 900, 800W/m^2$ when $t = 1, 2, 3, 4s$ respectively, SOC is 45%, and the total simulation time is $5s$

The related results of photovoltaic output power P_{pv} and load power P_l are shown in Figure 7. The P_{pv} will be changed accordingly according to the adjustment of light intensity S, while the P_l is about $22kW$. When the difference between P_{pv} and P_l is too large, the system will be unstable, and the battery is needed to smooth the power fluctuation and achieve the stability of the bus voltage.

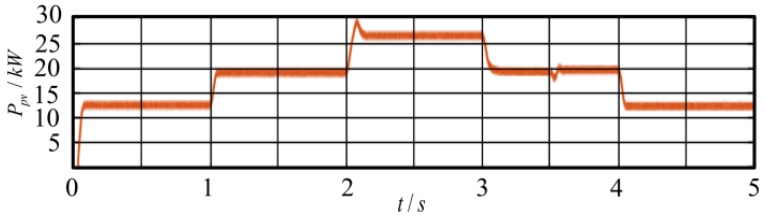

(a) Photovoltaic output power

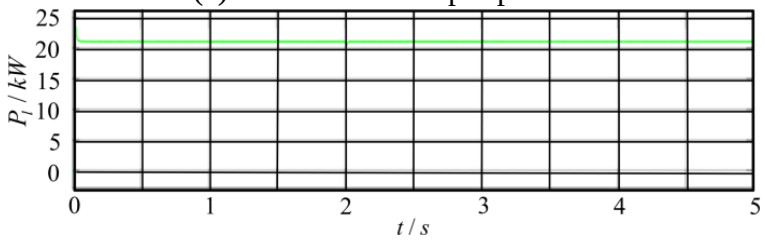

(b) Load power

Figure 7 Simulation diagram of photovoltaic power generation and load power consumption

The simulation results of battery output power can be seen in Figure 8. Compared with Figure 7, $P_l > P_{pv}$ within 0~2s, at which time battery discharge is required to compensate the power difference between P_{pv} and P_l. When the light intensity is $1000W/m^2$, the photovoltaic output with the maximum power of $25kW, P_{pv} > P_l$ within 2 ~ 3s, the battery is required to absorb excessive power.

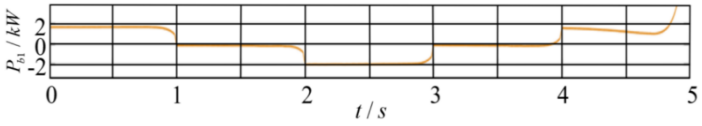

Figure 8 Simulation diagram of power waveform of storage battery

The DC bus voltage can be seen in Figure 9. From the figure, it can be seen that the voltage fluctuation time is not long and eventually stabilizes around the set value. The voltage deviation range of each time period when the condition changes is less than 5%, which is stable within the allowable range.

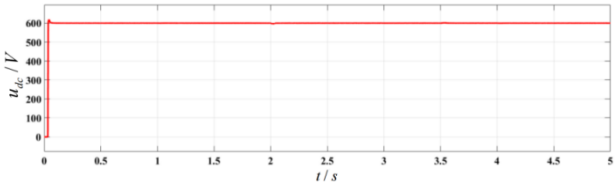

Figure 9 Bus voltage waveform

(3) State 5

Setting $\mathrm{T} = 25℃$, the light intensity $S = 800,\ 900W/m^2$ when $t = 0,\ 1s$ respectively, SOC is 20%, and the total simulation time is $3s$.

Figure 10 shows the experimental results of photovoltaic output power P_{pv}, load consumption power P_l and bus voltage u_{dc}. As can be seen from the figure, the P_l basically remains at $22kW$

before $t = 2s$, and P_{pv} is always smaller than P_l although it fluctuates due to the change of light intensity S; The battery has been discharged and can not meet the load power, so consider cutting off some unnecessary loads P_{load1} and P_{load2} when $t = 2s$, to balance the system energy and maintain the fluctuation deviation of the bus voltage in the standard range.

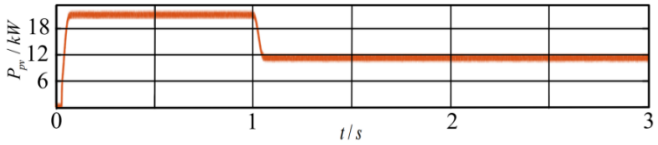

(a) Photovoltaic power

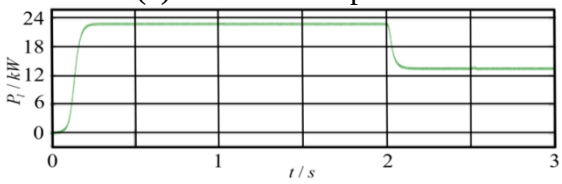

(b) Load consumption power

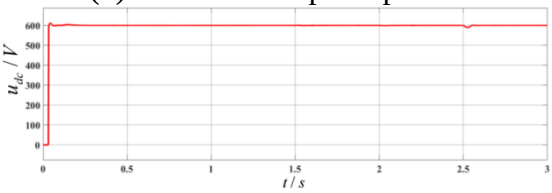

(c) Bus voltage

Figure 10 The experimental results of photovoltaic output power, load consumption power and bus voltage

To analyzing the operation characteristics of P_{pv} after change shows that the method proposed in this paper can balance the internal power of the system and maintain the stability of the bus voltage in various operation modes of DC microgrid.

3.2.2 Analysis of operating characteristics when the total load power changes

Setting P_{pv} to be constant for a certain period of time, when the load P_l changes to P_{l1}. At this time, when $t = 1s$, the accessed load power changes from $P_{load} = 12kW$ to $P_{1load} = 14kW$, and load $P_{load1} = 6kW$ is accessed at $t = 2s$, and load $P_{load2} = 4kW$ is accessed at $t = 3s$.

(1) State 1

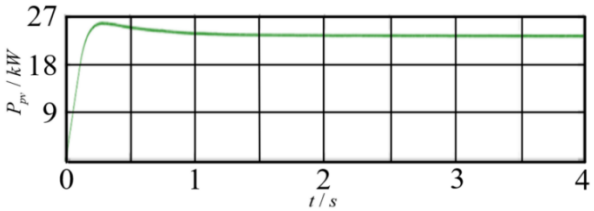

(a) Photovoltaic power

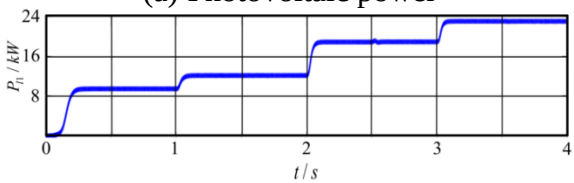

(b) Load consumption power

Figure 11 The simulation diagram of photovoltaic output power and load power

Setting $T = 25℃, S = 1000W/m^2, SOC = 20\%$, and the total simulation time is $4s$. Figure 11

shows the simulation diagram of photovoltaic output power P_{pv} and load power P_{l1}. The battery is in the two-stage charging state, and the photovoltaic unit is in the constant voltage mode.

(2) State 2/3/4

Setting $\mathrm{T} = 25℃, S = 900W/m^2, SOC = 50\%$, and the total simulation time is $4s$. The simulation results of P_{pv} is shown in Figure 12. It can be seen from the figure that when the light intensity S is unchanged, the P_{pv} remains at $20kW$. In the different stages of the experiment, the system power M and H are not equal, so it is necessary to use the battery to stabilize the bus voltage.

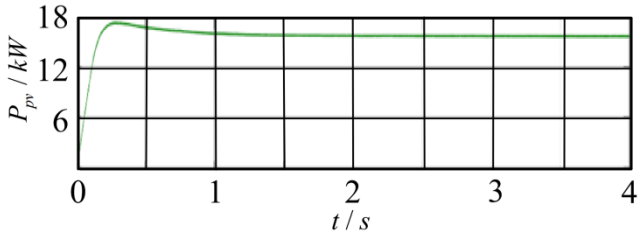

Figure 12 Photovoltaic power waveform

When P_{l1} is less than P_{pv} between 0 and 3s, the battery is in a charging state and stores excess energy. When P_{l1} is greater than P_{pv} between 3 and 4s, the battery discharge is used to balance the system power and maintain the energy balance state. The output voltage and output current of the battery are shown in Figure 13.

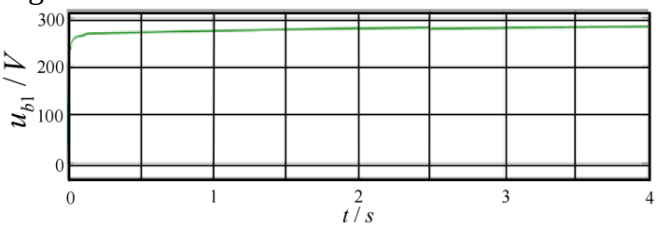

(a) Output voltage waveform of storage battery

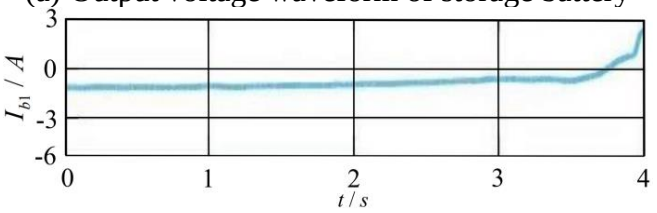

(b) Battery output current waveform of storage battery

Figure 13 The output voltage and output current of the battery

By means of the coordinated control between the battery and photovoltaic unit, the system's energy achieves equilibrium, leading to the stabilization of bus voltage, as depicted in Figure 14.

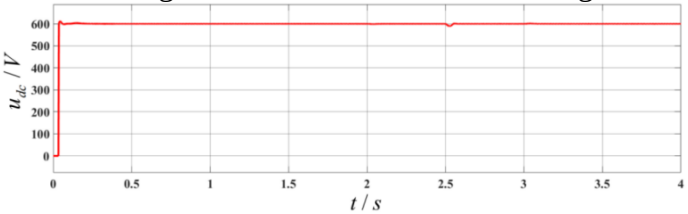

Figure 14 Bus voltage waveform

(3) State 5

Setting $\mathrm{T} = 25℃, S = 800W/m^2, SOC = 20\%$, and the total simulation time is $5s$. Figure 15 shows the simulation results of photovoltaic output power and bus voltage. It can be seen from the

figure that when the light intensity is unchanged, the P_{pv} remains around $13kW$. When the battery is in the overdischarge state and still cannot meet the power required by the load, consider cutting off part of the unimportant $P_{load1}, P_{load2}$when $\mathrm{t} = 4s$ to balance the system energy, so that the bus voltage fluctuates within the range required by the guidelines.

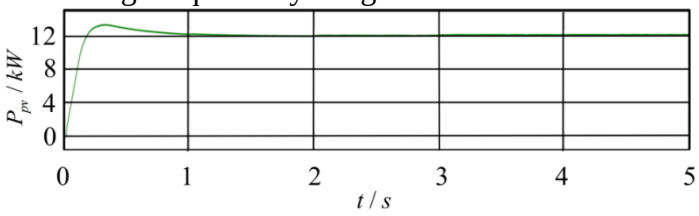

(a) Photovoltaic power waveform

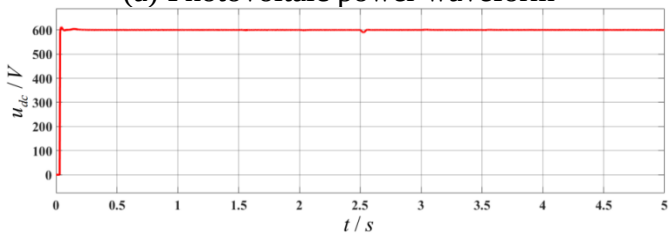

(b) Photovoltaic power waveform

Figure 15 The simulation results of photovoltaic output power and bus voltage

4. Conclusion

In this study, focusing on bus voltage u_{dc}, photovoltaic output power P_{pv}, and load power P_l, various operational modes of the photovoltaic-energy storage DC microgrid were categorized. The investigation and analysis were conducted for scenarios where abrupt changes occur in P_{pv} and P_l. The stability of the system after these impact scenarios was subsequently validated. Analysis of experimental results reveals that when the microgrid operates in State 1, the photovoltaic units are in a constant voltage mode. In State 2/3/4, the battery's charging and discharging are utilized to dampen power fluctuations. Upon entering State 5, if the battery's discharge does not meet the power gap required by the load, the battery ceases discharge while disconnecting non-essential loads to maintain power balance. Throughout all operational states of the microgrid, the proposed coordinated control method ensures power balance, stabilizes voltage, and ultimately guarantees the safe and economical operation of the system.

References

[1] Tah A, Das D. An enhanced droop control method for accurate load sharing and voltage improvement of isolated and interconnected DC microgrids [J]. IEEE Transactions on Sustainable Energy, 2016, 7(3):1194-1204.

[2] Merabet A, Labib L, Ghias A M Y M. Robust model predictive control for photovoltaic inverter system with grid fault ride-through capability [J]. IEEE Transactions on Smart Grid, 2017, 9(6):5699-5709.

[3] Zuo K, Wu L. A review of decentralized and distributed control approaches for islanded microgrids: Novel designs, current trends, and emerging challenges [J]. The Electricity Journal, 2022, 35(5): 107138.

[4] Munteanu D, Marinescu C, Serban I, et al. Control of PV inverter with energy storage capacity to improve microgrid dynamic response [C] //2016 International Conference on Applied and Theoretical Electricity (ICATE). IEEE, 2016, 26(12):1-5.

[5] Jianguo L, Biao Z, Qiang S, et al. DC Transformer Based on Switched Capacitor in High and Medium Voltage DC Power System [J]. Transactions of china electrotechnical society, 2018, 14(10):714-722.

[6] Zhang Xueyin, Xu Yonghai, Xiao Xiangning. A High Power Density Resonance Cascaded H-Bridge Solid-State Transformer for Medium and High Voltage Distribution Network [J]. Transactions of China Electrotechnical Society, 2018, 14(10):714-722.

[7] Li Q, Peng C, Chen M, et al. Networked and distributed control method with optimal power dispatch for islanded

microgrids [J]. IEEE Transactions on Industrial Electronics, 2016, 64(1):493-504.
[8] Kenzelmann S, Rufer A, Dujic D, et al. Isolated DC/DC Structure Based on Modular Multilevel Converter [J]. IEEE Transactions on Power Electronics, 2017, 30(1):89-98.
[9] Yu Chen, Shanshan Zhao, Zuoyu Li, et al. Multi-Object Control of an Isolated DC-DC Modular Multilevel Converter (DC-DC MMC) for Medium Voltage Direct Current (MVDC) Grids [J]. Iet Power Electronics, 2018, 11(8): 1338-1349.
[10] Muhammad Naveed Naz, Muhammad Irfan Mushtaq, Muhammad Haneef. Multicriteria decision making for resource management in renewable energy assisted microgrids [J]. Renewable and Sustainable Energy Reviews, May 2017, 14(10):323-341.